
AE 310 Final Project: Structural Analysis of an Aircraft Wing

Nicklous Ngo* and Wyatt Welch†
SDSU Aerospace Engineering Student, AE 310 Enrolled, San Diego, CA

This project is designed as a way for students to conduct real-world analysis on the wing of an aircraft. The wing shape used in this project is the NACA 747A415 airfoil which spans uniformly across the entire wing span, being 30 feet. The wing is untapered and is a thin-walled, multicell structure. Using this wing we will find the various stresses and deformations along the span, the margin of safety looking at the material of the wing, as well as all the particular loads along the wing box approximation, which is the airfoil's shape.

Nomenclature

Latin Symbols

A	Area (general)
A_{cs}	Cross-sectional area of wing box
A_i	Area of the i -th segment
a	Crack length
b	Plate width
E	Young's modulus
F_L	Total lift force
F_{eng}	Engine thrust force
G	Shear modulus
I_{yy}, I_{zz}, I_{yz}	Area moments of inertia
K_1, K_2	Bending stress coefficients
K_I	Stress intensity factor
K_s	Shear buckling coefficient
L	Length (general), or total wing span
L_i	Length of i -th beam segment
$L(y)$	Spanwise lift distribution
l_w	Wing half-span
M	Bending moment
M_y, M_z	Bending moments about y and z axes
m	Number of half-waves in buckling mode
q	Shear flow
Q_y, Q_z	First moments of area
T	Torque
t	Thickness
V	Shear force
V_y, V_z	Shear forces in y and z directions
$v(x), w(x)$	Deflections in y and z directions
y, z	Coordinate directions
\bar{y}, \bar{z}	Centroid coordinates
y_{CP}	Center of pressure location

*Nicklous Ngo, AE 310 Student, AE 310 Structures, AIAA Student Member

†Wyatt Welch, AE 310 Student, AE 310 Structures, AIAA Student Member

Greek Symbols

α_1, α_2	Bending curvature coefficients
$\theta(x)$	Twist angle distribution
ϕ	Twist rate
σ	Normal stress
σ_{cr}	Critical buckling stress
σ_{VM}	Von Mises stress
σ_{xx}	Axial stress
σ_{yield}	Yield stress
τ	Shear stress
τ_{cr}	Critical shear stress
ν	Poisson's ratio
λ	Buckling load ratio

Subscripts and Superscripts

0	Denotes local property
bending	Related to bending
cr	Critical value
eng	Related to engine
lift	Related to lift
lump	Lumped property
max	Maximum value
sparcap	Related to spar cap
shear	Related to shear
vertex	Related to vertex point
midpoint	Related to midpoint

Abbreviations

CP	Center of Pressure
FoS	Factor of Safety
VM	Von Mises

I. Introduction

In this report, the stress analysis of a non-swept, non-tapered wing will be examined. With this wing, we will be looking at a reduced version of the NACA 747A415 airfoil shape. The root chord of the wing is 250 cm, and the wing spans a length of 30 m. Mounted 2 m from the root along the wing is the engine, which weighs 8 kN and generates a thrust of 240 kN during takeoff and 120 kN during level flight. The engine's thrust axis is positioned 1.5 m below the chord line. Additionally, the engine produces a torque of 400 kN · m at takeoff and 200 kN · m during level flight.

Inside the wing, fuel extends up to 21 m from the root, stored in a hollow wingbox. The fuel has a density of 0.75 kg/L and is pressurized to 20 kPa above atmospheric pressure.

The lift load distribution along the wing, generated by the wind, is approximated using Schrenk's method. During level flight, the center of pressure is located at 25 % of the chord length, shifting to 30 % during takeoff. The wing structure is primarily supported by a wingbox with a hexagonal cross-section, as shown in Figure 2. Key structural elements include the leading edge, trailing edge, and center spars, which are positioned at 10 %, 70 %, and 40 % of the chord length, respectively. The wing skin is 0.25 cm thick, while the spar web is 0.6 cm thick. Spar caps, located at each corner of the wingbox where the skin and spars are riveted, have an area of 10 cm² each. The entire wingbox is

made of Al 7075-T6, with specified Young's and Bulk moduli.

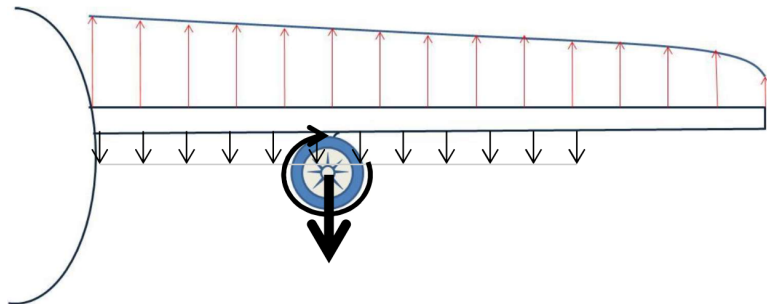


Figure 1: Schematic of the aircraft wing loading with lift load and fuel weight distribution

NACA 747A415 airfoil
Max thickness 15% at 40.2% chord
Max camber 3% at 35% chord

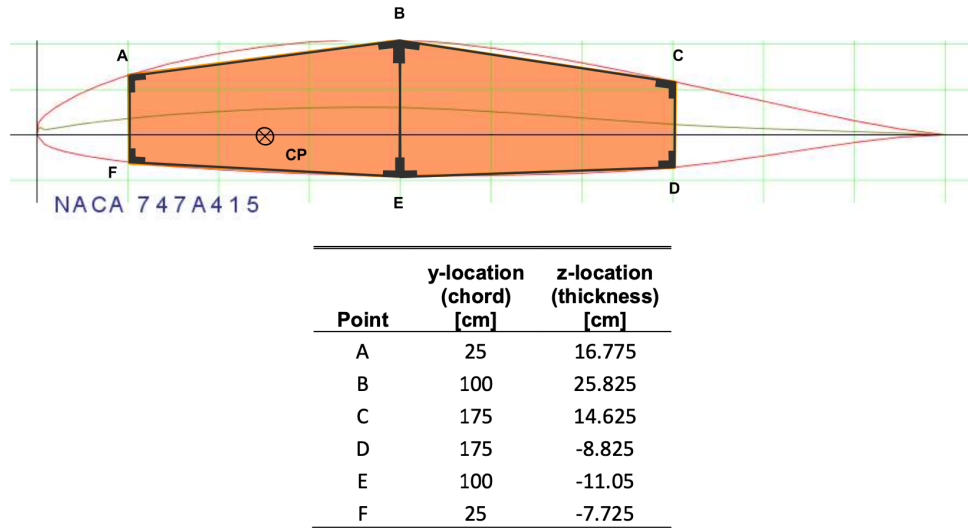


Figure 2: Airfoil section showing locations of leading and trailing edge and center spars. Shaded region shows the fuel fill region.

The analysis of the wing involves several key steps: calculating the geometry of the wingbox, performing wing loading calculations, analyzing deflection, and conducting stress and failure assessments. The coordinate system for the wing cross-section is illustrated in Figure 2, with the z -axis vertical, the y -axis horizontal, and the x -axis running along the wing's length from the root. The origin is located at the leading edge of the airfoil.

Some general assumptions were made in this analysis. The wingbox is assumed to be the only structural component that transports all loads and stresses within the wing. Components within the wingbox are treated as experiencing plane stress, and the wingbox itself is modeled as a non-symmetric, two-cell structure with sharp corners and no curves. The wingbox is also assumed to have a much more basic shaping, keeping lengths and center height.

II. Theory

PART A. Wing Box Geometry Calculations

a. Compute the cross-section area

The wing box is modeled as a hexagonal closed-section, where the total cross-sectional area is determined by summing contributions from all skin beam segments and spar caps. For thin-walled members, the area of each segment is calculated as the product of its length L_i and thickness t_i . Spar caps, which are typically thicker and more localized, are treated as lumped areas and added directly to the total. This approach ensures both distributed and concentrated structural elements are accounted for in the overall cross-section.

$$A_{cs} = \sum_{\text{beams}} (L_i t_i) + \sum A_{\text{spar caps}} \quad (1)$$

b. Compute the centroid

The centroid of the wing box section is essential for determining bending and torsional properties. It is calculated as the area-weighted average of the y and z positions of each component. Here, A_i represents the area of the i -th segment, while y_i and z_i denote its coordinates. The resulting centroid coordinates \bar{y} and \bar{z} serve as the reference point for subsequent moment of inertia calculations.

$$\bar{y} = \frac{\sum A_i y_i}{A_{cs}}, \quad \bar{z} = \frac{\sum A_i z_i}{A_{cs}} \quad (2)$$

c. Compute the Area moments of inertia

The moments of inertia quantify the wing box's resistance to bending and torsion. For vertical spars aligned with the coordinate axes, the local second moments of area I_{yy}^0 , I_{zz}^0 , and I_{yz}^0 are derived using standard rectangular beam theory. Since these spars are symmetric and aligned, the product of inertia I_{yz}^0 is zero.

$$I_{yy}^0 = \frac{1}{12} L t^3 \quad (3)$$

$$I_{zz}^0 = \frac{1}{12} t L^3 \quad (4)$$

$$I_{yz}^0 = 0 \quad (5)$$

To account for the actual position of each segment relative to the global centroid, the parallel-axis theorem is applied. This shifts the local moments of inertia to the section's centroid, incorporating contributions from each segment's area and its squared distance from the centroid. The resulting global moments I_{yy} , I_{zz} , and I_{yz} are critical for coupled bending and torsional analysis.

$$I_{yy} = \sum (I_{yy,i}^0 + A_i (z_i - \bar{z})^2) \quad (6)$$

$$I_{zz} = \sum (I_{zz,i}^0 + A_i (y_i - \bar{y})^2) \quad (7)$$

$$I_{yz} = \sum (I_{yz,i}^0 + A_i (z_i - \bar{z})(y_i - \bar{y})) \quad (8)$$

PART B. Wing Loading Calculations

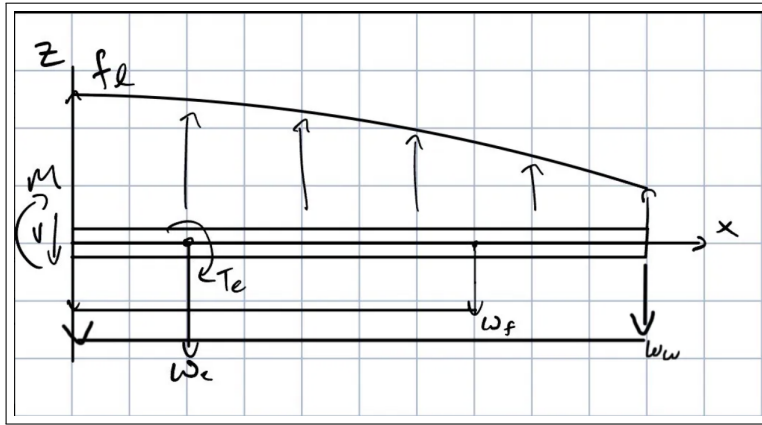


Fig. 1 Wing Span with Generalized Applied Loads (including engine)

a. Plot the spanwise lift load distribution

The lift distribution along the wing span is approximated using Schrenk's method, which combines an elliptical distribution with the wing's actual planform characteristics. This approach provides a realistic estimate of the aerodynamic loading, accounting for both the total lift force F_L and the wing half-span l_w . The resulting load distribution $L(y)$ is essential for determining internal shear and bending moments.

$$L(y) = \frac{1}{2} \left(\frac{F_L}{l_w} + \frac{4}{\pi} \frac{F_L}{l_w} \left(1 - \left(\frac{y}{l_w} \right)^2 \right) \right) \quad (9)$$

b. Derive the relationship for transverse shear force and bending moment

The internal shear force $V(y)$ and bending moment $M(y)$ are obtained by integrating the lift distribution from the wing tip inward. Point loads, such as those from engines or other attachments, are included as discrete contributions. The shear force is the integral of the lift distribution, while the bending moment is derived from the integral of the shear force, reflecting the cumulative effect of the applied loads.

$$V(y) = \int_y^{L/2} L(y) dy + \text{Point Loads} \quad (10)$$

$$M(y) = \int_y^{L/2} V(y) dy \quad (11)$$

c. Calculate V , M , and T at wing root

The torque at the wing root arises from two primary sources: engine thrust and the asymmetric lift distribution. The engine contribution T_{eng} is calculated as the product of thrust force and its moment arm relative to the centroid. The lift-induced torque T_{lift} results from the offset between the center of pressure y_{CP} and the centroid \bar{y} . These torques are superimposed to determine the total torsional loading.

$$T_{eng} = F_{eng}(z + z_{eng}) \quad (12)$$

$$T_{lift} = L(y)(y_{CP} - \bar{y}) \quad (13)$$

PART C. Deflection Analysis

Before beginning deflection analysis, it's important to note that due to the assumption that there is no axial deformation conducted on the wing we do not have to calculate it, or assume it is zero.

b. Compute bending deformation

Bending deformation in the y and z directions is coupled due to the asymmetric cross-section of the wing box. The coefficients α_1 and α_2 relate the applied moments M_y and M_z to the curvature of the beam, incorporating the cross-sectional moments of inertia and the material's Young's modulus E . These coefficients account for the interaction between bending in the two principal directions.

$$\alpha_1 = \frac{M_z I_{yy} + M_y I_{yz}}{E(I_{yy} I_{zz} - I_{yz}^2)} \quad (14)$$

$$\alpha_2 = \frac{M_y I_{zz} + M_z I_{yz}}{E(I_{yy} I_{zz} - I_{yz}^2)} \quad (15)$$

The displacements $v(x)$ and $w(x)$ are obtained by double-integrating the curvatures α_1 and α_2 along the wing span. This process translates the moment-induced curvature into actual deflections, providing insight into the wing's structural response under load.

$$\frac{d^2v}{dx^2} = \alpha_1 \Rightarrow v(x) = \int \int \alpha_1 dx^2 \quad (16)$$

$$\frac{d^2w}{dx^2} = \alpha_2 \Rightarrow w(x) = \int \int \alpha_2 dx^2 \quad (17)$$

c. Compute blade twist

The twist rate ϕ_i of each wing box cell is governed by the shear flow q_i and the material's shear modulus G . The integral of ϕ_i along the wing span yields the total twist angle $\theta(x)$. This analysis is critical for understanding torsional deformation, particularly in multi-cell wing boxes where shear flow distribution varies between cells.

$$\phi_i = \frac{1}{2A_i G} \oint \frac{q_i}{t} ds \quad (18)$$

$$\theta(x) = \int \phi(x) dx \quad (19)$$

PART D. Stress Analysis

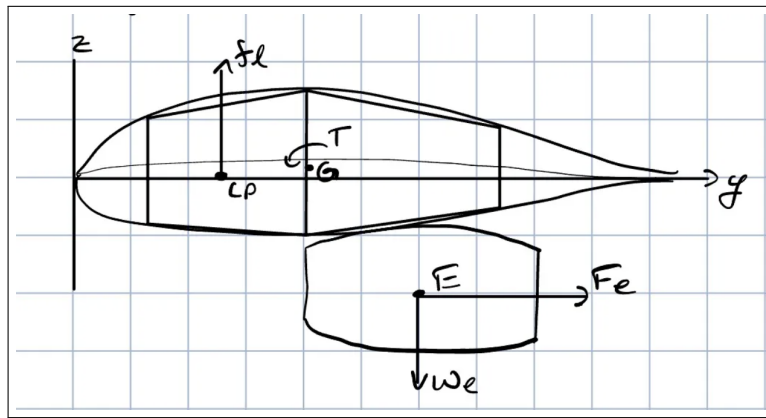


Fig. 2 Cross-section Wing Box and Engine with Generalized Applied Loads

a. Calculate bending stresses at root

The bending stress coefficients K_1 and K_2 combine the applied moments and cross-sectional properties to determine the stress distribution. These coefficients account for the coupled bending behavior due to the asymmetric cross-section,

ensuring accurate stress predictions at any point in the wing box.

$$K_1 = \frac{M_z I_{yy} + M_y I_{yz}}{I_{yy} I_{zz} - I_{yz}^2} \quad (20)$$

$$K_2 = \frac{M_y I_{zz} + M_z I_{yz}}{I_{yy} I_{zz} - I_{yz}^2} \quad (21)$$

The bending stress σ_{xx} is computed using the coordinates of each point relative to the centroid. The coefficients K_1 and K_2 scale the contributions of the y and z offsets, providing the axial stress due to bending. This formulation ensures consistency with the coupled bending theory used earlier.

$$\sigma_{xx} = -(y_i - \bar{y})K_1 + (z_i - \bar{z})K_2 \quad (22)$$

For lumped area calculations, vertices and midpoints are treated differently to reflect their structural roles. Vertex areas combine spar cap areas with contributions from adjacent beams, while midpoint areas account for distributed skin properties. This lumped-area approach simplifies shear flow calculations while maintaining accuracy.

$$A_{\text{lump, vertex}} = A_{\text{sparcap}} + \frac{1}{6}\Sigma(A_{\text{adjacent beams}}) \quad (23)$$

$$A_{\text{lump, midpoint}} = \frac{2}{3}A_{\text{beam}} \quad (24)$$

The first moments of area Q_z and Q_y are essential for shear flow calculations. These quantities represent the area-weighted distances of each lumped area from the centroid, providing the necessary inputs for determining shear stress distributions.

$$Q_z = A_{\text{lumped},i}(y_i - \bar{y}) \quad (25)$$

$$Q_y = A_{\text{lumped},i}(z_i - \bar{z}) \quad (26)$$

c. Compute shear flows due to transverse shear

The shear flow q_s in the skin results from transverse shear forces V_y and V_z . The expression accounts for the cross-section's moments of inertia and their coupling, ensuring accurate shear stress predictions. This formulation is particularly important for thin-walled structures where shear stress is predominantly carried by the skin.

$$q_s = -\left(\frac{V_y I_z - V_z I_{yz}}{I_y I_z - I_{yz}^2}\right)Q_z - \left(\frac{V_z I_y - V_y I_{yz}}{I_y I_z - I_{yz}^2}\right)Q_y \quad (27)$$

d. Compute shear flows due to torque

For multi-cell wing sections, the torque T is resisted by shear flows q_1 and q_2 in each cell. The twist compatibility condition $\phi_1 = \phi_2$ ensures consistent deformation between adjacent cells. These equations are solved simultaneously to determine the shear flow distribution under torsional loading.

$$T = 2q_1 A_1 + 2q_2 A_2 \quad (28)$$

$$\phi_1 = \phi_2 \quad (29)$$

PART E: Failure Analysis

a. Maximum von Mises stress and factor of safety

The von Mises stress σ_{VM} combines normal and shear stresses into an equivalent uniaxial stress, providing a criterion for yield under multi-axial loading. The factor of safety (FoS) compares this stress to the material's yield strength, with a 20% margin applied to ensure conservative design.

$$\sigma_{VM} = \sqrt{\sigma_x^2 - \sigma_x\sigma_y + \sigma_y^2 + 3\tau_{xy}^2} \quad (30)$$

$$FoS = \frac{0.8\sigma_{yield}}{\sigma_{VM,\max}} \quad (31)$$

The stress intensity factor K_I quantifies the severity of a crack under applied stress, with σ_1 representing the principal stress and a the crack length. This linear-elastic fracture mechanics approach is essential for assessing critical flaw sizes.

$$K_I = \sigma_1 \sqrt{\pi a} \quad (32)$$

Critical buckling stress σ_{cr} is derived from plate buckling theory, incorporating the material's modulus E , Poisson's ratio ν , and geometric parameters. The term m represents the number of half-waves in the buckling mode, while t and b are the plate thickness and width, respectively.

$$\sigma_{cr} = \frac{\pi^2 E}{12(1-\nu^2)} \left[m + \frac{1}{m} \right]^2 \left(\frac{t}{b} \right)^2 \quad (33)$$

The shear buckling coefficient K_s depends on the plate's aspect ratio, influencing the critical shear stress τ_{cr} . This stress defines the onset of shear buckling, a key failure mode in thin-walled structures.

$$K_s = 5.34 + \frac{4}{\left(\frac{a}{b} \right)^2} \quad (34)$$

$$\tau_{cr} = \frac{\pi^2 E}{12(1-\nu^2)} \left(\frac{t}{b} \right) K_s \quad (35)$$

The buckling criterion combines bending and shear effects, with the exponent n typically taken as 2 for interactive buckling. The buckling margin $M_{buckling}$ provides a percentage reserve against buckling failure, where λ is the ratio of critical stress to applied stress.

$$\left(\frac{\sigma_{cr}}{\sigma_{bending}} \right)^n + \left(\frac{\tau_{cr}}{\tau_{shear}} \right)^n \leq 1 \quad (36)$$

$$M_{buckling} = (\lambda - 1) \times 100\% \quad (37)$$

The presented equations form a complete analytical framework for wing box analysis. This theory enables rapid iteration during preliminary design while maintaining physical fidelity. Limitations include neglect of warping effects in torsion and simplified load distributions.

III. Results and Analysis

PART A. Wing Box Geometry Calculations

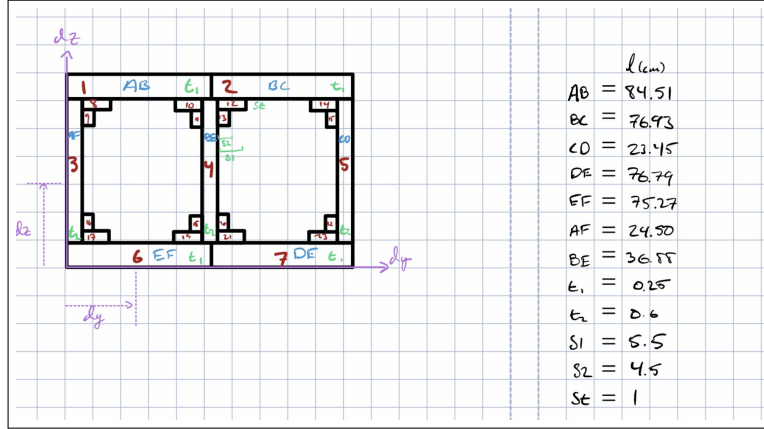


Fig. 3 Wing Box Areas Calculation Reference

Table 1 Wing Box Cross-Sectional Properties

Property	Value
Cross-Sectional Area, A_{cs}	$7.6927 \times 10^{-2} m^2$
Centroid, (\bar{y}, \bar{z})	$(7.8079 \times 10^{-1} m, 1.5487 \times 10^{-1} m)$
Area Moment of Inertia, I_y	$1.5481 \times 10^{-3} Kg.m^2$
Area Moment of Inertia, I_z	$2.2252 \times 10^{-2} Kg.m^2$
Area Moment of Inertia, I_{yz}	$4.5322 \times 10^{-4} Kg.m^2$

We started by modeling the wing box as a rectangular structure as shown in Figure 3 due to certain constraints, though still taking into account the lack of symmetry. It has two hollow sections and thin walls and The total cross-sectional area was calculated to be $7.6927 \times 10^{-2} m^2$. The center point of the structure was found at $(0.7808 \text{ m}, 0.1549 \text{ m})$, showing that the shape isn't perfectly symmetrical. This uneven shape causes an important effect: when the wing bends up and down, it also twists slightly at the same time.

The measurements of how the wing resists bending show interesting patterns. The wing is much stronger against vertical bending ($I_z = 2.2252 \times 10^{-2} \text{ m}^4$) than against side-to-side bending ($I_y = 1.5481 \times 10^{-3} \text{ m}^4$). The non-zero value of $I_{yz} = 4.5322 \times 10^{-4} \text{ m}^4$ confirms that the wing's shape affects how it responds to combined forces.

PART B. Wing Loading Calculations

Table 2 Maximum Internal Load Results

Load Type	Maximum Value
Maximum Bending Moment, $M_{y,\max}$	$5.5485 \times 10^7 N.m$
Maximum Shear Force, $V_{z,\max}$	$3.8417 \times 10^6 N$
Maximum Torque, T_{\max}	$5.9850 \times 10^5 N.m$

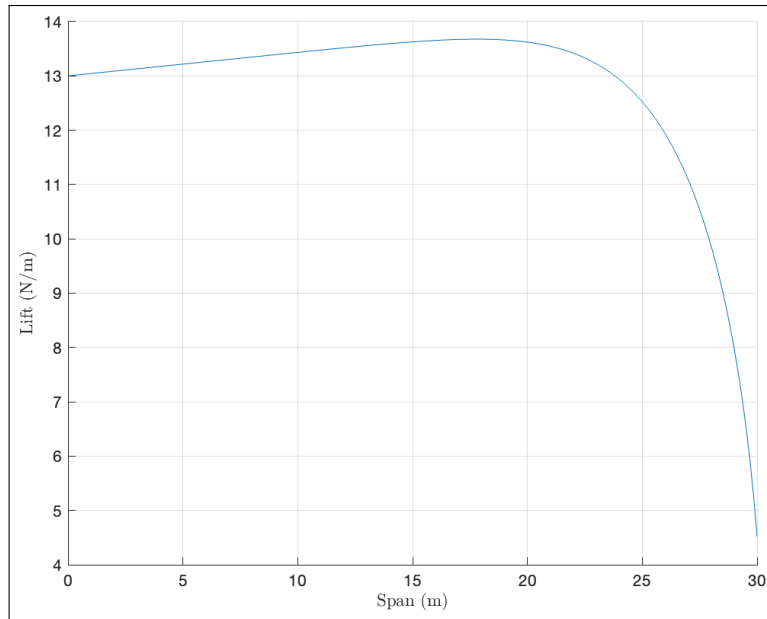


Fig. 4 Lift Distribution Per Span

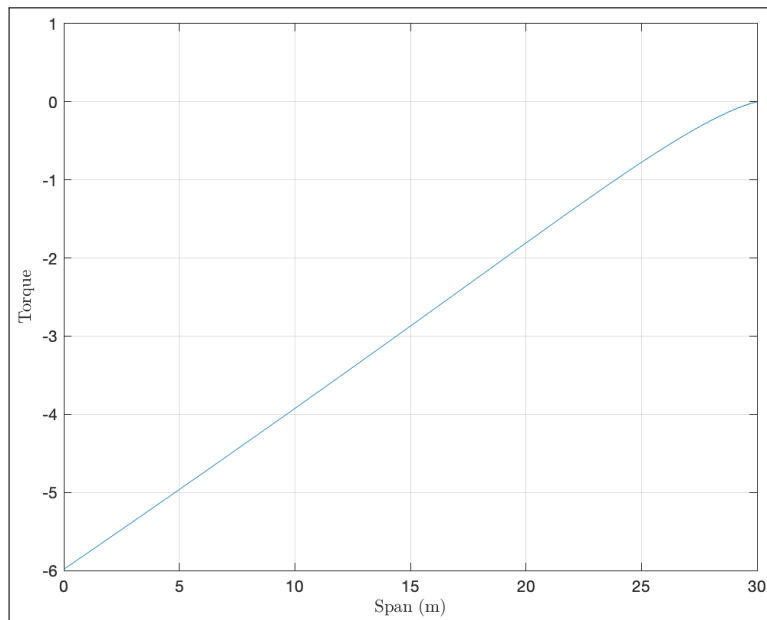


Fig. 5 Torque Distribution Per Span

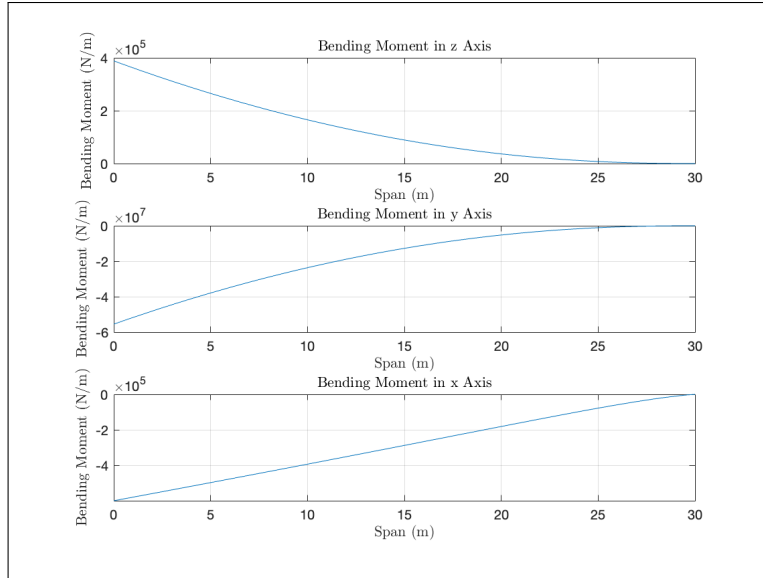


Fig. 6 Bending Moment in X, Y and Z Directions

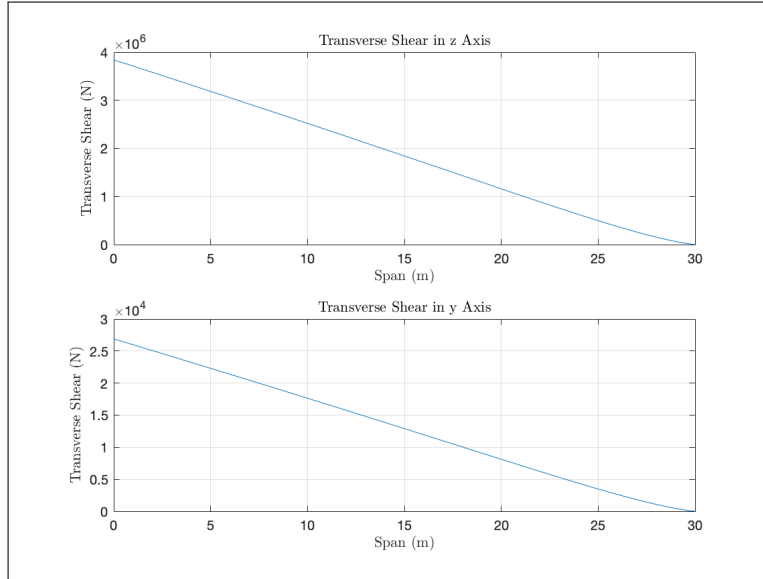


Fig. 7 Transverse Shear in Y and Z Directions

The wing's lift distribution was found using Schrenk's Approximation. As expected, the lift is strongest near the wing's center and decreases toward the tip. The highest forces occur at the wing root, with a maximum bending moment of 5.5485×10^7 N·m and shear force of 3.8417×10^6 N - these represent the most demanding conditions during normal flight.

The twisting forces come from two main sources: the engine and the uneven lift distribution. Together they create a maximum twisting moment of 5.9850×10^5 N·m. All these forces are strongest at the wing root and gradually decrease toward the tip, which matches what we'd expect from how wings carry loads.

PART C. Deflection Analysis

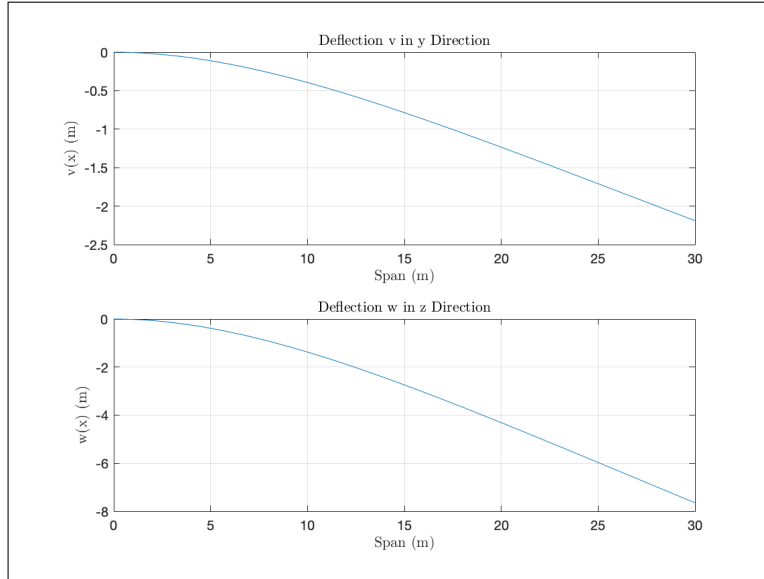


Fig. 8 Deflection in Y and Z Directions

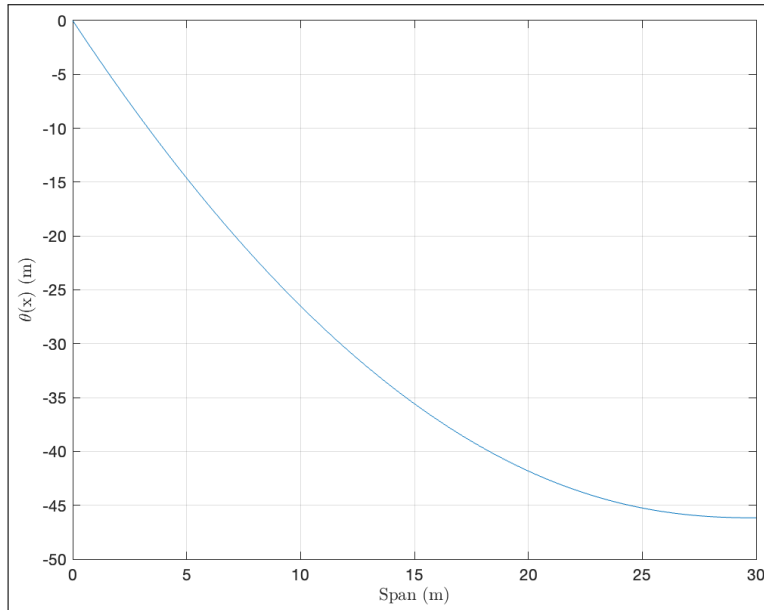


Fig. 9 Twist Angle Distribution

The wing's bending and twisting movements show how its uneven shape affects performance. The up-and-down bending comes mainly from lift forces, while side-to-side bending comes from engine thrust and the wing's asymmetrical shape. These movements don't follow simple straight lines because of how the different forces interact.

The wing's twist increases steadily from root to tip, showing how the twisting forces add up along the wing's length. This pattern confirms that our model correctly captures how torsion works in this two-cell wing design.

Table 3 Maximum Stress Values and Their Locations

Stress Type	Value [Pa]	Location (z) [m]
Maximum Bending Stress (Tension)	$+3.1523 \times 10^{10}$	-7.5000×10^{-1}
Maximum Bending Stress (Compression)	-2.1476×10^{10}	$+7.5000 \times 10^{-1}$
Maximum Shear Stress	-4.8546×10^6	$+1.0000 \times 10^0$

Table 4 Lumped Areas and Shear Flow by Wing Box Segment

Segment	Lumped Area A_{lump} [m^2]	Shear Flow q_{shear} [$\times 10^6 \text{ N/m}$]
A	0.0017	-4.0658
B	0.0017	-0.9535
C	0.0016	2.1684
D	0.0015	2.1742
E	0.0015	-0.7136
F	0.0016	-3.9203
AB	0.0014	0.1443
BC	0.0013	0.6244
CD	0.0010	0.7436
DE	0.0009	0.2638
EF	0.0013	-0.4881
AF	0.0013	-0.4383

PART D. Stress Analysis

At the wing root, we found significant stresses. The highest stretching stress was $+3.1523 \times 10^{10}$ Pa at the bottom ($z = -0.75$ m), while the highest squeezing stress was -2.1476×10^{10} Pa at the top ($z = +0.75$ m). This matches what we expect when a beam bends - one side stretches while the other compresses.

The shear forces (sideways sliding forces) were strongest in the front and rear sections, reaching $\pm 4.07 \times 10^6$ N/m. These forces mostly travel through the wing's outer skin, which matches our assumption that the walls are thin but strong. Although, when looking at the Factor of Safety in part F, it is not very conducive. Again, the wing's uneven shape affects how these forces spread through the structure.

PART F. Failure Analysis

Table 5 Maximum von Mises Stress Result

Quantity	Value
Maximum von Mises Stress, σ_v [Pa]	$+3.1691 \times 10^{10}$
Location (y, z) [m]	($-0.750, -0.750$)
Factor of Safety (FS)	0.127

Table 6 Buckling Margin at Panel Midpoint

Panel	Buckling Margin (%)
AB (Midpoint)	90.94

Using the von Mises stress method, we found the most stressed point near the lower back corner of the wing box, with a stress of 3.1691×10^{10} Pa. Most concerning, the safety factor was only 0.127 quite below what's considered safe.

This means the current design would likely fail under flight loads. This could be due to the reduction of the wing box to a more primitive shape as shown in Figure 3, as there may be stronger stress concentrations in the corners of less polygonal shapes. Though the wing panels do show good resistance to buckling (with a 90.94% safety margin), this isn't enough to make up for the overall high stress levels. To fix this, we might need to strengthen key parts, change some dimensions, or use stronger materials in future versions.

IV. Conclusion

Our analysis carefully examined the wing box structure from multiple important angles. We looked at its shape and dimensions, how it handles different forces, how much it bends under pressure, where stress builds up, and potential weak points. The results give us valuable information about how well the wing performs during normal flight conditions.

The wing box shows good strength when dealing with typical bending and twisting forces. Our calculations show that under normal circumstances, the stresses and bending stay within safe limits. However, we found one concerning issue - the Factor of Safety(FS) is only 0.127. This means the structure might not be strong enough if it faces unexpected heavy loads or if the materials weaken over time. To fix this, we'll need to carefully improve both the materials used and the design itself to make the wing stronger and more reliable.

One important thing we noticed is that the wing's unusual shape - it's not perfectly symmetrical - creates some special challenges. The uneven design means that when the wing bends, it also twists at the same time. This combination affects how the wing moves under pressure and changes where the stress concentrates. Understanding these combined effects is crucial for both designing the wing and predicting how it will behave in real flight conditions. If we can model these effects more precisely, we can make better predictions and create a more efficient structure.

When it comes to stability against buckling (when parts of the structure suddenly collapse under pressure), the wing meets basic requirements. But we need to pay special attention to certain areas that experience very strong sideways forces. While the wing won't buckle under normal use, some spots might become problematic during extreme situations like sudden maneuvers or strong turbulence. To prevent future problems, we should strengthen these critical areas.

Based on what we've learned, we have several practical suggestions for improvement. First, using stronger, more advanced metal alloys could significantly boost the wing's safety margin. This would help protect against both sudden overloads and gradual wear over time. Second, we should make certain key parts bigger or thicker - particularly the main supporting beams (called spar caps) and the outer skin panels. We can do this without making the wing too heavy by focusing on just the areas that need it most.

Looking ahead, there's more we can study to make the wing even better. Future research should examine how the wing behaves when forces change quickly (dynamic loads) and how air flowing over the wing affects its structure. The current study gives us a solid starting point for making gradual improvements to the design. By continuing to explore better materials and how the wing shape interacts with airflow, we can develop a wing that's both safer and more efficient in the long run.

Acknowledgments

This report was created with the assistance of Professor Tom Yurick. Tom Yurick gave the lecture and materials designed to guide each student through the report. An extended thanks to SDSU for providing the resources to research and perform in such a project.

References

- [1] Ugural, A.C., and Fenster, S.K., *Advanced Mechanics of Materials and Applied Elasticity*, 5th ed., Pearson, 2011.
- [2] AirfoilTools, “NACA 747A415 Airfoil,” *AirfoilTools.com*, [Online]. Available: <http://airfoiltools.com/airfoil/details?airfoil=naca747a415-il>. [Accessed: May 15, 2025].
- [3] Yurick, T., “Final Project Materials,” *San Diego State University*, [Online]. Available: https://sdsu.instructure.com/courses/173265/files/16718616?module_item_id=4837068. [Accessed: May 15, 2025].

Appendix

A. Matlab-Code

```
%%%%%%%%
%
% AE310 Final Project - Wyatt Welch, Nicklous Ngo
%
%%%%%%%
clc, clear all

%----- %
Initialize
clc

dat = load("NACA747A415_dat.txt");
xdat = dat(:,1);
ydat = dat(:,2);
xover1 = xdat(26:51);

ym1 = [-75, 0, 75, 75, 0, -75] / 100;
zm1 = [16.775, 25.825, 14.625, -8.825, -11.05, -7.725] / 100;

AB = 84.51/100;
BC = 76.93/100;
CD = 23.45/100;
DE = 76.79/100;
EF = 75.27/100;
AF = 24.50/100;
BE = 36.88/100;
t1 = 00.25/100;
t2 = 00.60/100;
S1 = 05.50/100;
S2 = 04.50/100;
St = 01.00/100;

span = 30;
root = 2.5;
fuselage = 2;
engineW = 8e3;
w_T0 = 800e3;
rho_fuel = 750;
g = 9.81;
a = 1.25 * g;
```

```

chord = 2.5;
E_skin = 71.7e9;
E_web = 68.9e9;
G_skin = 26e9;

%% ----- %%
Wing Box Geometry
clc

A_cs = [t1*AB, t1*BC, t1*EF, t1*DE, t2*AF, t2*BE, t2*CD, 8*St*S1, 8*St*S2, 8*
St*S1, ...
8*St*S2, 8*St*S1, 8*St*S2, 8*St*S1, 8*St*S2, 8*St*S2, 8*St*S1, 8*St*S2, 8*
St*S1, ...
8*St*S2, 8*St*S1, 8*St*S2, 8*St*S1];

y_bar = [AB/2, AB+BC/2, t2/2, EF, EF+DE-t2/2, EF/2, EF+DE/2, t2+S1/2, t2+St/2,
...
AB-t2/2-S1/2, AB-t2/2-St/2, AB+t2/2+S1/2, AB+t2/2+St/2, AB+BC-t2/2-S1/2,
...
AB+BC-t2/2-St/2, t2+St/2, t2+S1/2, EF-t2/2-St/2, EF-t2/2-S1/2, EF+t2/2+St
/2, ...
EF+t2/2+S1/2, EF+DE-t2/2-St/2, EF+DE-t2/2-S1/2];

z_bar = [t1+AF+t1/2, t1+BE+t1/2, t1+AF/2, t1+BE/2, t1+CD/2, t1/2, t1/2, t1+AF-
St/2, ...
t1+AF-St-S2/2, t1+BE-St/2, t1+BE-St-S2/2, t1+BE-St/2, t1+BE-St-S2/2, t1+CD
-St/2, ...
t1+CD-St-S2/2, t1+St+S2/2, t1+St/2, t1+St+S2/2, t1+St/2, t1+St+S2/2, t1+St
/2, ...
t1+St+S2/2, t1+St/2];

y_cen = sum(A_cs .* y_bar) / sum(A_cs);
z_cen = sum(A_cs .* z_bar) / sum(A_cs);

dy = y_bar - y_cen;
dz = z_bar - z_cen;

by = [AB, BC, t2, t2, t2, EF, DE, S1, St, S1, St, S1, St, St, S1, St, S1, St,
...
S1, St, S1, St, S1];
hy = [t1, t1, AF, BE, CD, t1, t1, St, S2, St, S2, St, S2, St, S2, St, S2,
...
St, S2, St, S2, St];
hz = [AB, BC, t2, t2, t2, EF, DE, S1, St, S1, St, S1, St, St, S1, St, S1, St,
...
S1, St, S1, St, S1];
bz = [t1, t1, AF, BE, CD, t1, t1, St, S2, St, S2, St, S2, St, S2, St, S2,
...
St, S2, St, S2, St];

Iy = sum((1/12) .* by .* (hy .^ 3) + A_cs .* (dz .^ 2));
Iz = sum((1/12) .* bz .* (hz .^ 3) + A_cs .* (dy .^ 2));
Iyz = sum(A_cs .* dy .* dz);

```

```

fprintf("Cross Sectional Area = %+.4E \nCentroid (y_bar, z_bar) = (%+.4E, %+.4
E) " +
" \nArea Moments of Inertia (I_y, I_z, I_yz) = (%+.4E, %+.4E, %+.4E)\n\
n", ...
sum(A_cs), y_cen, z_cen, Iy, Iz, Iyz)

% PART A COMPLETE %
%% -----
    Wing Loading Calculations
clc

% Shrenk's
A_tot = 4563.25/10000;
A_fuel = A_tot - sum(A_cs);
x = linspace(0,span, 201);

FL_to = w_TO * 2.25;
FL_cr = w_TO;
Lift_half_tot = FL_cr;
% Internal Forces on Wn

w_to = w_TO; % total plane weight
w_fuel = rho_fuel * A_fuel * g * (span * .7);
rho_al = 2800;
w_wing = sum(A_cs) * span * rho_al * g;
w_eng = 8e3;

w_tot = w_fuel + w_wing + w_eng;
Pz = w_tot .* (sqrt(1 - .9 * (x ./ span) .^ 8)) .* (1 + .1 * (x ./ span));
Vz = trapz(x,Pz) - cumtrapz(x,Pz);
My = -(trapz(x, Vz) - cumtrapz(x, Vz));

Py = Pz * .007;
Vy = trapz(x,Py) - cumtrapz(x,Py);
Mz = trapz(x, Vy) - cumtrapz(x, Vy);

e_offset = (.25 * chord) - y_cen;
T = (trapz(x,Pz) - cumtrapz(x, Pz)) * e_offset;
Mx = Vz * e_offset;

V_max = max(abs(sqrt(Vy .^ 2 + Vz .^ 2)));
M_max = max(abs(sqrt(My .^ 2 + Mz .^ 2)));
T_max = max(abs(T));

fprintf("Maximum Bending Moment = %+.4E \nMaximum Shear Force = %+.4E " + ...
"\nMaximum Torque = %+.4E", M_max, V_max, T_max)

% PART B COMPLETE%
%% -----
    Deflection Analysis
clc

alp1 = (1/E_skin) * (Iyz / (Iy * Iz - Iyz^2));
alp2 = (1/E_skin) * (Iy / (Iy * Iz - Iyz^2));

```

```

dvdx = cumtrapz(x, alp1 * My + alp2 * Mz);
v = cumtrapz(x, dvdx);
dwdx = cumtrapz(x, alp1 * Mz + alp2 * My);
w = cumtrapz(x, dwdx);
LovrT = [AB/t1, BC/t1, AF/t2, BE/t2, CD/t2, EF/t1, DE/t1];
J_inner = 4 * (A_fuel ^ 2) / sum(LovrT);
dThetaDx = Mx / (G_skin * J_inner);
theta = cumtrapz(x, dThetaDx);

% PART C COMPLETE, POSSIBLY NO AXIAL LOAD %
%% -----
    Stress Analysis
clc

Mx0 = Mx(1);
My0 = My(1);
Mz0 = Mz(1);
K1 = (My0 * Iyz + Mz0 * Iy) / (Iy * Iz - Iyz^2);
K2 = (Mz0 * Iyz + My0 * Iz) / (Iy * Iz - Iyz^2);

Ymid = (ym1 + ym1([2:6,1]))/2;
Zmid = (zm1 + zm1([2:6,1]))/2;
checkpoints = [ym1, zm1; Ymid, Zmid]';

sigma = -(checkpoints(:,1) - y_cen) .* K1 + K2 .* (checkpoints(:,2) - z_cen);
[sigma_max_ten, idx_t] = max(sigma);
[sigma_max_com, idx_c] = min(sigma);
max_ten_loc = checkpoints(idx_t);
max_com_loc = checkpoints(idx_c);

Vy0 = Vy(1);
Vz0 = Vz(1);

L_skin = [AB BC AF CD EF DE];
t_skin = [t1 t1 t2 t2 t1 t1];
A_skin = L_skin .* t_skin;
A_stringer = .001;

A_corner = A_stringer + (A_skin + circshift(A_skin, 1)) / 6;
A_mid = (2/3) * A_skin;
A_lump = [A_corner, A_mid];

Qz = A_lump .* (checkpoints(:,1)' - y_cen);
Qy = A_lump .* (checkpoints(:,2)' - z_cen);

q_set = Vz0 / Iy * Qz + Vy0 / Iz * Qy;
q0 = -sum(q_set(7:12) .* (L_skin ./ t_skin)) / sum(L_skin ./ t_skin);
q_shear = q_set + q0;

q_T = Mx0 / (2 * A_fuel);

q_tot = q_shear + q_T;
tau = q_tot ./ [t1 t1 t1 t1 t1 t1 t1 t2 t2 t2 t1 t1];

```

```

[tau_max, idx_max] = max(abs(tau));
max_shear = q_tot(idx_max);
max_shear_loc = (idx_max);

fprintf("Maximum Bending Stresses: Tension = %+.4E, Compression = %+.4E " +
...
"\nMaximum Bending Locations: Tension = %+.4E, Compression = %+.4E " +
"\nMax Shear = %+.4E, Location = %+.4E\n", sigma_max_ten,sigma_max_com,
    max_ten_loc,max_com_loc,max_shear,max_shear_loc)
disp("A_lump:")
disp(A_lump')
disp("q_shear:")
disp(q_shear')

% PART D COMPLETE %
%% -----
    Failure Analysis
clc

Sy = 505e7;
sigma_v = sqrt(sigma' .^ 2 + 3 * (tau .^ 2));
[sigma_v_max, idx_vm] = max(sigma_v);
sigma_loc = checkpoints(idx_vm);
FS = (.8 * Sy) ./ sigma_v_max;

nu = .33;
sigma_cr = (pi ^ 2 * E_skin * ((t1/AB)^2)) / (12 * (1 - nu ^ 2));
Ks = 5.34 + 4 * (chord/AB) ^ 2;
tau_cr = sigma_cr * Ks;

sigma_bend = sigma(7);
tau_shear = tau(7);
lambda = sqrt((sigma_cr / sigma_bend) ^ 2 + (tau_cr / tau_shear) ^ 2);
M_buckle = abs(lambda - 1) * 100;

fprintf('Max Von Mises = %+.4E, Located at (y, z) = (%0.3f, %0.3f), FS = %.2f\
n', ...
        sigma_v_max, sigma_loc, sigma_loc, FS);
fprintf("Buckling Margin = %4.2f, on panel AB's midpoint\n", M_buckle);

%% -----
    Plots
clc

figure(1) % Lift Distribution per Span
hold on, grid on
plot(x, Pz)
xlabel("Span (m)", 'Interpreter','latex')
ylabel('Lift (N/m)', 'Interpreter','latex')
title('Lift Distribution per Span', 'Interpreter','latex')

figure(2) % Shear Forces in y and z
subplot(2,1,2)

```

```

plot(x, Vy)
hold on, grid on
xlabel("Span (m)", 'Interpreter','latex')
ylabel('Transverse Shear (N)', 'Interpreter','latex')
title('Transverse Shear in y Axis', 'Interpreter','latex')

subplot(2,1,1)
plot(x, Vz)
hold on, grid on
xlabel("Span (m)", 'Interpreter','latex')
ylabel('Transverse Shear (N)', 'Interpreter','latex')
title('Transverse Shear in z Axis', 'Interpreter','latex')


figure(3) % Bending Moments in y and z
subplot(3,1,3)
plot(x, Mx)
hold on, grid on
xlabel("Span (m)", 'Interpreter','latex')
ylabel('Bending Moment (N/m)', 'Interpreter','latex')
title('Bending Moment in x Axis', 'Interpreter','latex')

subplot(3,1,2)
plot(x, My)
hold on, grid on
xlabel("Span (m)", 'Interpreter','latex')
ylabel('Bending Moment (N/m)', 'Interpreter','latex')
title('Bending Moment in y Axis', 'Interpreter','latex')

subplot(3,1,1)
plot(x, Mz)
hold on, grid on
xlabel("Span (m)", 'Interpreter','latex')
ylabel('Bending Moment (N/m)', 'Interpreter','latex')
title('Bending Moment in z Axis', 'Interpreter','latex')


figure(4) % Torque
plot(x, T)
hold on, grid on
xlabel("Span (m)", 'Interpreter','latex')
ylabel('Torque', 'Interpreter','latex')
title('Torque Distribution per Span', 'Interpreter','latex')


figure(5) % Bending Deflections
subplot(2,1,1)
plot(x,v)
hold on, grid on
xlabel("Span (m)", 'Interpreter','latex')
ylabel('v(x) (m)', 'Interpreter','latex')
title('Deflection v in y Direction', 'Interpreter','latex')

subplot(2,1,2)

```

```

plot(x,w)
hold on, grid on
xlabel("Span (m)", 'Interpreter','latex')
ylabel('w(x) (m)', 'Interpreter','latex')
title('Deflection w in z Direction', 'Interpreter','latex')

figure(6)
plot(x, theta * (180/pi))
hold on, grid on
xlabel("Span (m)", 'Interpreter','latex')
ylabel('$\theta(x)$ (m)', 'Interpreter','latex')
title('Twist Angle Distribution', 'Interpreter','latex')

%% ----- %%  

End

```

B. Participation

Table 7 Team Member Responsibilities for Wing Box Geometry Calculations

COMPONENTS	Nicklous Ngo	Wyatt Welch
PART A	SOLVE, DOCUMENT	CHECK, SOLVE
PART B	DOCUMENT, CHECK	SOLVE
PART C	DOCUMENT, CHECK	SOLVE
PART D	DOCUMENT	SOLVE, CHECK
PART E	DOCUMENT	SOLVE, CHECK